Physics of the Earth and Planetary Interiors xxx (2008) xxx–xxx

Contents lists available at ScienceDirect

Physics of the Earth and Planetary Interiors

journal homepage: www.elsevier.com/locate/pepi

Subsidence in intracontinental basins due to dynamic topography

Christian Heine[a,*], R. Dietmar Müller[a], Bernhard Steinberger[b], Trond H. Torsvik[b,1]

[a] EarthByte Group, School of Geosciences, The University of Sydney, NSW 2006, Australia
[b] Center for Geodynamics, Norges Geologiske Undersøkelse (NGU), Trondheim, Norway

ARTICLE INFO

Article history:
Received 16 November 2007
Received in revised form 8 May 2008
Accepted 20 May 2008

Keywords:
Intracontinental basins
Crustal structure
Anomalous tectonic subsidence
Dynamic topography
Plate motions

ABSTRACT

The origin of anomalous tectonic subsidence (ATS) of large intracontinental basins long after their most recent phase of extension and last thermal perturbation is the subject of a long standing debate. We show that deep-Earth processes may contribute to the subsidence of these tectonically stable basins by analysing the Tertiary mantle convection-driven topography history of a global set of more than 220 intracontinental basins, integrated into a plate kinematic framework. Most basins are affected by increasing negative dynamic topography over the last 70 Myr, due to the motion of many continents away from large mantle upwellings and towards downwellings previously located along the perimeter of the supercontinent Pangaea. During continental dispersal, increasing negative dynamic topography causes dynamic subsidence of the basins, creating additional accommodation space. We utilise a parameter from a global crustal analysis of intraplate basins, termed "anomalous tectonic subsidence", to quantify sediment accumulation not related to crustal stretching. We propose that dynamic subsidence due to plate motions relative to the underlying mantle, as well as variations in the large-scale convection patterns can significantly contribute to the creation (and destruction) of accommodation space in intraplate basins.

1. Introduction

Intracontinental basins are archives for the long-term vertical motions of the Earth's crust, both for mantle- and crustal-scale processes. Many attempts have been made to explain the evolution of large, long-lived sedimentary basins which are located in plate interiors, relatively isolated from the effects of active plate boundary deformation. These basins are mostly old structures, saucer-shaped in cross section and related to fossil rifts in continental platforms or tectonically stable continental interiors (Fig. 1; Şengör, 1995; Artyushkov, 1992; Milanovsky, 1992). They have been subsiding over long periods of time without showing signs of brittle deformation. They also display a characteristically low topography (e.g. Illinois, Taoudeni, West Siberian Basins; Vyssotski et al., 2006; Klein, 1995; Hartley and Allen, 1994; Khain, 1992; Milanovsky, 1992; Sleep, 1976). The last main phase of active extension or thermal disturbance in most of these basins is significantly older than 100 Ma, hence thermal subsidence related to the extensional event can be ruled out as a major subsidence mechanism, as, for example, demonstrated for the Chad basin in Central Africa (Hartley and Allen, 1994). Different hypotheses attempting to explain the long-lasting subsidence of these basins have been proposed, which can be grouped into five main, mutually non-exclusive categories: (1) lithospheric stretching and thermal contraction; (2) crustal and mantle phase changes; (3) changes in the in-plane stress field; (4) convective instabilities; and (5) sub-aerial erosion following a thermal uplift. See Klein (1995) and Hartley and Allen (1994) for a summary and review. However, these hypotheses fail to explain the observed subsidence patterns of large intracontinental basins within a coherent global geodynamic framework.

Lithgow-Bertelloni and Gurnis (1997); Gurnis et al. (1998) and Gurnis (2001, 1990) demonstrated that the relative position of continents with respect to large-scale mantle up- and downwellings causes uplift and subsidence of the Earth's surface ("dynamic topography"). Tilted stratigraphic sequences covering the stable North American continent during the Phanerozoic (Sloss, 1963; Bond, 1976, 1978; Sleep, 1976) suggest periods of continent-scale trans- and regressional cycles which cannot be explained by a rise in eustatic sea level alone, but instead require large-scale tectonic mechanisms (Burgess and Gurnis, 1995; Lithgow-Bertelloni and Gurnis, 1997; Gurnis, 1993). Recent stud-

* Corresponding author at: StatoilHydro, Global Exploration Technology, Dramensveien 264, N-0240 Oslo, Norway.
E-mail address: christian@geosci.usyd.edu.au (C. Heine).
[1] Also at PGP, University of Oslo, Norway, and School of Geosciences, University of Witwatersrand, South Africa.

0031-9201/$ – see front matter © 2008 Elsevier B.V. All rights reserved.
doi:10.1016/j.pepi.2008.05.008

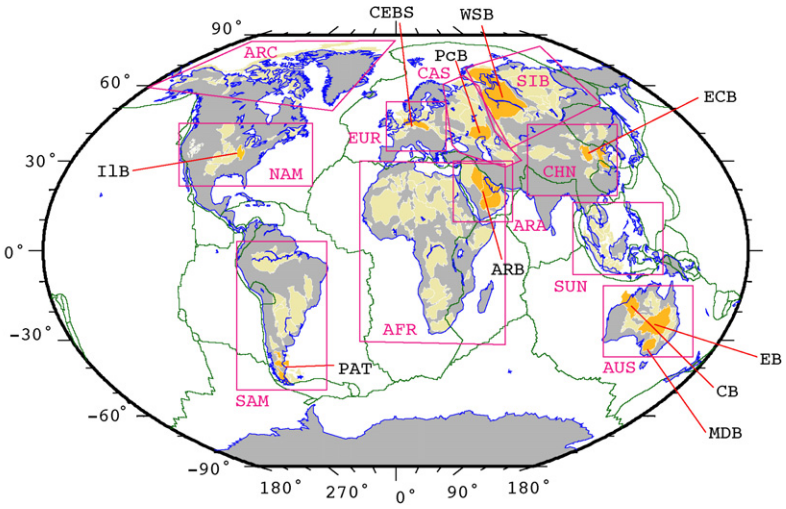

Fig. 1. Global map of basins which have been used for this study (light yellow). Abbreviations are: ARB, Arabian Basins; CB, Canning Basin (Australia); CEBS, Central European Basin System; EB, Eromanga Basin (Australia); ECB, Eastern Chinese Basins; MDB, Murray-Darling Basin (Australia); IlB, Illinois Basin; PAT, Patagonian Basins (South America); PcB, Precaspian Basin (Russia); WSB, West Siberian Basin (Russia). Magenta polygons denote region outlines as used in this study. Green lines denote plate boundaries (Bird, 2003).

ies suggest that dynamic topography has significantly affected the flooding history and stratigraphic record of eastern North America (Müller et al., 2008b; Kominz et al., 2008; Spasojevic et al., 2008).

Investigating the global Phanerozoic subduction history, Anderson (1994) pointed out that throughout the Mesozoic to Cenozoic distinct belts of plate convergence existed where subduction tends to repeat. This belt extends from the Arctic via North, Central and South America to Antarctica, and back via Australia, SE Asia/W Pacific, and eastern Eurasia, with an extension up to the eastern Mediterranean, following the former Tethyan subduction zone. These regions of convergence reflect first order patterns of mantle convection with cold material injected back into the deeper mantle, whereas two regions centered on southernmost Africa and the South Pacific represent superswells, with hotter material upwelling. This general picture has been confirmed by recent global seismic tomographic studies (Grand et al., 1997; Lithgow-Bertelloni and Silver, 1998; Ritsema et al., 2004). When supercontinents assemble, they insulate the mantle and isolate it from subduction (Anderson, 1994; Davies, 1999). Subsequent dispersal moves the continental fragments relative to mantle convection patterns towards the subduction zones, where they spend a prolonged period of time over downwelling oceanic lithosphere (Gurnis and Zhong, 1991; Anderson, 1994). Klein (1995) summarises observations which point to global commonalities of the formation and subsidence patterns of cratonic basins, likely related to the supercontinent cycles.

This paper investigates the effects of mantle convection-induced vertical displacement of intracontinental basins related to plate kinematics. We derive the subsidence or uplift history of a set of selected intracontinental basins for the last 70 Myr using combined dynamic topography model output and a self-consistent absolute plate motion reference frame. The amount of vertical motion is then compared to a parameter called anomalous tectonic subsidence (ATS), which quantifies subsidence in each given sedimentary basin not conforming to uniform crustal stretching models. We refer to this additional, mantle-induced subsidence as *anomalous tectonic subsidence*, as it originates in deep-Earth instead of lithospheric or tectosphere processes. We establish a relationship between basin ages, plate motion history and mantle convection-induced subsidence.

2. Data and models

2.1. Intracontinental basins

For our study, we utilise a set of about 229 basins selected from an global basin-polygon database. These basins were chosen based on the general criteria to encompass tectonically inactive, intracontinental basins on stable continental crust. They are located away from recently active plate boundaries and not situated on continental margins. Depending on the basin classification scheme, most, but not all basins are classified as interior sag or interior fracture (Kingston et al., 1983), intracontinental composite, interior, or complex basins (Klemme and Ulmishek, 1991; Klemme, 1980). All basins have in common a low topographic relief and an elevation close to present-day sea level (Fig. 2).

2.2. Crustal structure data

The global crustal structure model CRUST2 has been used to compute stretch factors and tectonic subsidence. The model has an original grid cell resolution of $2^\circ \times 2^\circ$ (Bassin et al., 2000; Laske, 2004) and consists of 7 layers, including the bottom of hard sedi-

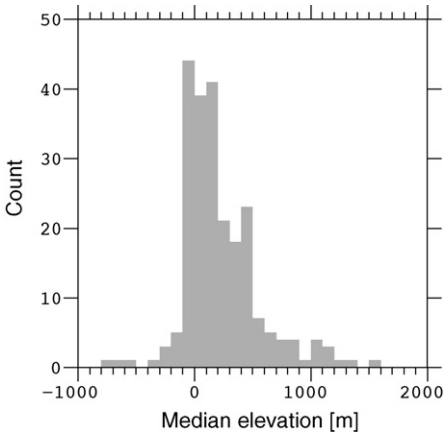

Fig. 2. Median elevation histogram for the selected basins of this study. Most basins are located around sea level.

Please cite this article in press as: Heine, C., et al., Subsidence in intracontinental basins due to dynamic topography, Phys. Earth Planet. Interiors (2008), doi:10.1016/j.pepi.2008.05.008

ments (= top basement) and the bottom of the lower crust (= Moho). Crustal thicknesses are reported to be within 5 km of true crustal thickness (Laske, 2004).

A $1^\circ \times 1^\circ$ sediment thickness grid by Laske and Masters (1997) is used as sediment thickness input for our computations. The grid is a compilation of sediment thickness data from various sources, including the Exxon Tectonic Map of the World (Exxon Production Research Company, 1985). Sediment thicknesses within each cell are reported to be within 1.0 km of true sediment thickness.

2.3. Dynamic topography model

Large-scale convection in the Earth's mantle is imaged by seismic tomographic models. The spatial distribution of relative seismic velocity highs and lows is inferred to correlate with the thermal mantle structure and is thought to be related to cold downwellings and hot upwellings. Both can dynamically alter the topography of the overlying boundary layer by either pushing it up above upwellings or drawing it down above downwellings.

We compute time-dependent surface topography for the last 70 Myr by advecting mantle density anomalies back through time in the mantle-flow field using a well-established global mantle convection modelling approach (Steinberger et al., 2004). The global S20RTS seismic tomographic model (Ritsema et al., 1999) is used to derive the density heterogeneities, using a conversion factor 0.25 from relative seismic velocity to density variations below depth 220 km. The factor 0.25 is based on a good fit with the observed geoid and also consistent with mineral physics (Karato, 1993; Steinberger and Calderwood, 2006). It assumes that both seismic velocity and density anomalies in the sub-lithospheric mantle are due to temperature anomalies, and hence perfectly correlated. The upper 220 km have been excluded from the model as seismic velocity anomalies might be to a large part due to compositional rather than thermal variations within the lithosphere. As dynamic topography is very sensitive to density variations at lithospheric depths, the exclusion of a heterogeneous lithosphere should avoid gross overestimation of dynamic topography amplitudes (Steinberger et al., 2001; Steinberger, 2007). However, in some regions, lithospheric keels and compositional heterogeneities might extend deeper than 220 km and partly cause over-prediction of the dynamic topography from mantle-flow models. See Steinberger (2007) for a discussion on the differences between various modelling results using different seismic tomography model input. The computed dynamic topography is relative to the geoid, i.e. relative to sea level.

The flow field of the mantle for the last 70 Myr is calculated using the spectral method described by Hager and O'Connell (1981), based on spherical harmonic expansion of surface plate velocities and internal density heterogeneities at each depth level (Steinberger et al., 2004; Xie et al., 2006; Steinberger and Calderwood, 2006). The flow model is constrained by matching paleo-latitudes of hotspots from paleomagnetic data.

We limit backward advection to the past 70 Myr. This is about the time span for which present-day mantle structure can be adequately reconstructed through a forward-convection model run, starting from the backward-advected model (Conrad and Gurnis, 2003). From the backward-advected density models, dynamic topography was computed beneath air with the same viscosity structure with high-viscosity lithosphere (2.4×10^{22} Pa s^{-1}), but with a free upper boundary, for a density contrast of 3.3 g/cm^3, corresponding to mantle density. The viscosity model (Steinberger et al., 2004) considers only radial viscosity variations and is based on mineral physics and obtains a good fit with the geoid and other observations.

Despite some shortcomings of the backward-advection model, it currently represents the best way that is practically applicable to predict dynamic topography on a global scale for Cenozoic times. Fig. 3 shows the present-day global dynamic topography based on conversion of seismic velocity anomalies for the S20RTS seismic tomography model (Ritsema et al., 1999) and includes the location of subduction zones for the last 140 Myr.

2.4. Plate kinematic framework

The plate kinematic framework which has been used for this work is based on a moving hotspot absolute plate motion reference frame (O'Neill et al., 2005) extended to 140 Ma as described in Müller et al. (2008a, b). It is in the following referred to as EarthByte model.

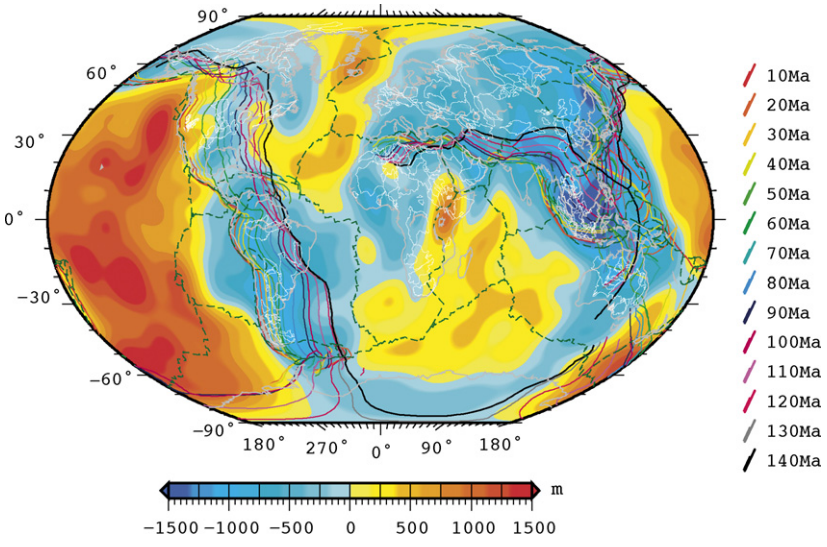

Fig. 3. Present-day dynamic topography and paleo-subduction zone locations. Dynamic topography is computed from S20RTS model (Ritsema et al., 2004). Paleo-subduction zone locations are generated from the EarthByte plate kinematic model (Müller et al., 2008a, b) and cover the last 140 Ma. Superimposed are intracontinental sedimentary basins of this study.

Please cite this article in press as: Heine, C., et al., Subsidence in intracontinental basins due to dynamic topography, Phys. Earth Planet. Interiors (2008), doi:10.1016/j.pepi.2008.05.008

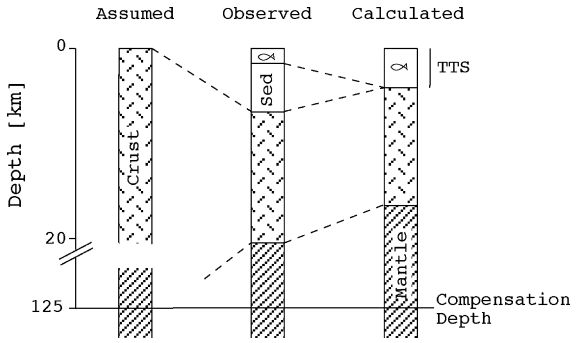

Fig. 4. Total tectonic subsidence. It is assumed that pre-extensional crust is at sea level. During stretching, crust thins and subsides with sediments filling the basin and loading the crust creating additional subsidence. To obtain the total amount of tectonic subsidence, the sediments are removed (backstripped) and the basement is unloaded. The total tectonic subsidence is equivalent to the water depth that would overlay the crust if no sediments had been deposited. The isostatic compensation depth is assumed to be at the base of the lithosphere (modified after Sawyer, 1985).

3. Crustal structure-based subsidence estimates in intracontinental basins

Our crustal structure-derived subsidence estimates are based on two computations: the total extension (extension factor β) within a given basin polygon and the total tectonic subsidence (TTS). Both were calculated individually using sediment thickness grids as well as basement crustal thickness according to the CRUST2 model for all basins to quantify extension and subsidence. Global data sets allow computation of these simple estimates of crustal and lithospheric extension under the assumption of a simple uniform extension, pure-shear model (McKenzie, 1978).

However, different extensional mechanisms like depth-dependent stretching or simple shear might be invoked alternatively to explain subsidence of sedimentary basins. These depend on the regional tectonic environment at a given time when the basin is evolving, compositional and rheological differences in the lithosphere, and pre-existing heterogeneities. Sediment thickness data to compute stretching estimates provide lithospheric stretching estimates whereas crustal thickness data will only yield crustal stretching factors.

3.1. Total tectonic subsidence

The total amount of subsidence in a basin is defined as the sum of sediment thickness above a basement horizon and the water depth (Fig. 4). Sawyer (1985) defined the term "total tectonic subsidence" as the difference between the pre-rifting continental crust elevation and the present, *sediment unloaded*, basement depth in a sedimentary basin. Although the TTS contains less information than subsidence history analysis, it can be applied to multiple points in a basin and is thus ideal for basin-wide, or even continent-wide analysis of data points.

Most intracontinental basins are currently found at low elevations and display evidence of mostly continental and shallow water deposition. Hence the total subsidence equates to the sediment thickness. We assume that the basement surface was at sea level when the basin started forming. To obtain the tectonic subsidence from the sediment thickness, it is necessary to backstrip the sediments and unload the basement (Fig. 4). The unloading correction U requires to make assumptions about the sediment thickness and average density as well as the crustal response to spatially and temporarily varying sediment load. Generally the unloading equation takes the form of:

$$U = t_s \frac{\bar{\rho}_s - \rho_w}{\rho_m - \rho_w} \quad (1)$$

where U is the unloading correction, t_s the observed sediment thickness, $\bar{\rho}_s$ the average sediment density of the whole sequence, ρ_m the mantle density and ρ_w the density of sea water. Typically U is about 2/3 of the sediment thickness.

It is assumed here that the crust is in local Airy isostatic equilibrium and has no flexural rigidity. As most of the basins have a diameter well over 300 km, the Airy isostatic compensation model is a good approximation to investigate large-scale basin subsidence anomalies (Watts, 2001).

Sawyer (1985) has shown that flexural loading and a local isostatic model will be similar in regions where the sediment has nearly uniform lateral thickness as the flexural isostatic correction is a function of sediment thickness at all nearby points. Most of the intracontinental basins used in this study are broad depressions, hence they show laterally relatively uniform distribution of sediment thicknesses.

3.2. Subsidence estimates from sediment thickness

Total tectonic subsidence estimates can be derived using the thickness and average density of the sediments in each given basin.

For computing the isostatic response of the crust due to sediment loading/unloading we follow Sykes' approach (Sykes, 1996) to compute the average density of a sediment column of a given thickness based on a density–depth relationship derived from Ocean Drilling Program (ODP) data.

$$\mathrm{IsC} = 0.43422\, t_s - 0.010395\, (t_s)^2 \quad (2)$$

where t_s is the observed sediment thickness at any given point in the basin and IsC is the isostatic correction. The differences in isostatic correction between using this approach or a uniform sediment density can exceed 2000 m for thick sedimentary sequences (10–12 km; Sykes, 1996).

To compute the tectonic subsidence inferred from the sedimentary infilling, the unloading correction based on the formula of

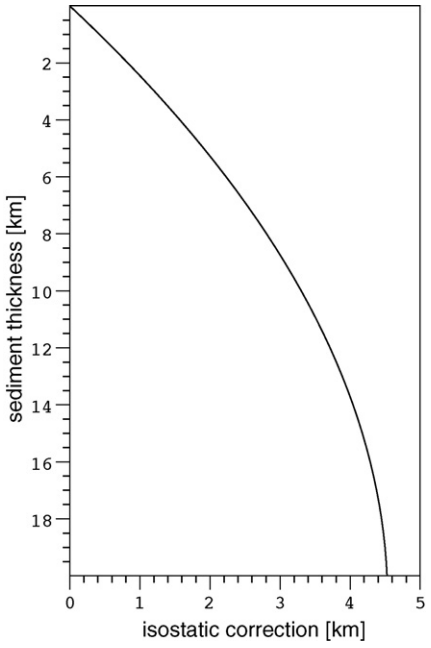

Fig. 5. Total tectonic subsidence thickness versus isostatic correction using Sykes (1996).

Please cite this article in press as: Heine, C., et al., Subsidence in intracontinental basins due to dynamic topography, Phys. Earth Planet. Interiors (2008), doi:10.1016/j.pepi.2008.05.008

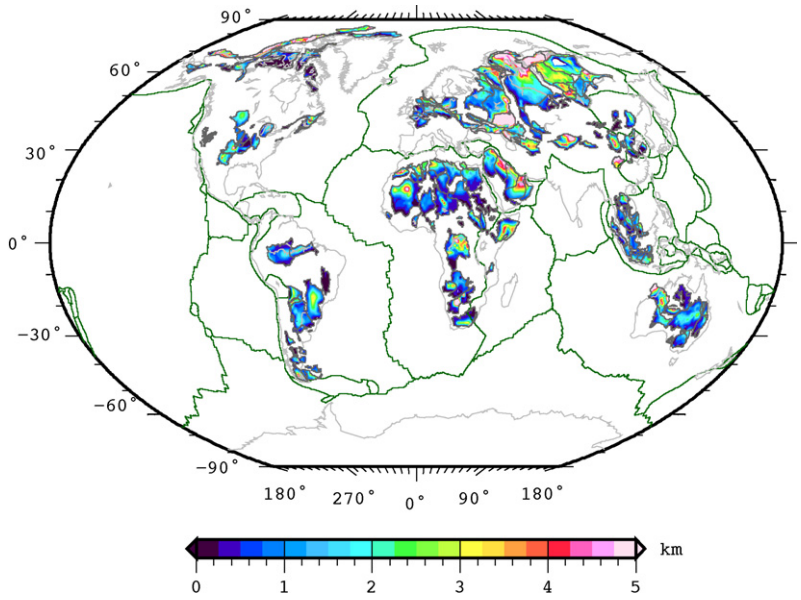

Fig. 6. Global map of total tectonic subsidence derived from sediment thickness (TTS_{sed}) for selected basins of this study.

Sykes (1996) (Eq. (2) and Fig. 5) is subtracted from the observed basement depth. Theoretically, this should restore the basement to the surface, if no additional tectonic forces acted on the basin. The grids for TTS_{sed} are computed using:

$$TTS_{sed} = t4 - IsC \quad (3)$$

where $t4$ is the base of the hard sediments according to the CRUST2 model and IsC is the isostatic correction derived using Eq. (2).

The global TTS_{sed} map (Fig. 6) indicates values of larger than 1.5 km for more than 50 intracontinental basins globally, with a median value of 0.7 km. Most basins show a circular pattern, indicating more tectonic subsidence in the basin center.

3.3. Subsidence estimates from basement thickness

Crustal stretching factor grids were computed by calculating the basement crustal thickness BCT (CRUST2 Moho depth minus CRUST2 Base hard sediments). If the crust and lithosphere are thinned uniformly, the principle of isostasy requires the surface to subside (McKenzie, 1978; Turcotte and Schubert, 2001; Allen and Allen, 2005). The McKenzie (1978) *pure-shear* model assumes that the crustal volume stays constant during the process as do the crustal densities. For accurate regional estimation of crustal extension factors, it was assumed that the median thickness of the basin rim (the outline of a given basin) represents the most objective input for an initial, pre-rifting crustal thickness estimate relative to the observed crustal thickness in the basin interior. However, as erosion is most likely concentrated at the basin rim, we here assume a "no-erosion" end member scenario, implying minimised stretch factor estimates and reduced tectonic subsidence due to cooling.

The median thickness along the individual basin rims was extracted from the basement thickness grid and used as initial crustal thickness relative to the BCT grid of the basin interior. The crustal extension factor for the basins in the study was calculated for the individual basins according to this equation:

$$\beta_{crust} = \frac{t_{rim}}{t_c} \quad (4)$$

where t_{rim} is the median crustal thickness along the basin rim and t_c is the BCT in the interior of the basin.

The TTS based solely on basement crustal thickness (TTS_{cru}) can be derived using the equation of Le Pichon and Sibuet (1981) in Sawyer (1985) and Allen and Allen (2005) and the extension factors derived from the basement thickness (β_{cru}):

$$TTS_{cru} = 7.82\,km \cdot \left(1 - \frac{1}{\beta_{cru}}\right) \quad (5)$$

where TTS_{cru} is the total tectonic subsidence of the crust, and β_{cru} is the crustal extension factor (Eq. (4)).

The highest TTS_{cru} values (>3 km) are observed in the basins extending from the interior of a continent onto the offshore margins, like the Australian Canning Basin, the West Siberian Basin, the Patagonian Basins, and some North American Arctic basins (Fig. 7, for locations see Fig. 1). The Global median value for crustal tectonic subsidence is 0.3 km. The Australian Eromanga Basin and Murray-Darling Basins, the Timan-Pechora Basin west of the northern Ural Mountains in Russia, and the Texan Permian Basin, Oklahoma and Illinois Basins show notable higher TTS_{cru} values as "true" intracontinental basins. These observations are well in agreement with published values (e.g. Artyushkov, 1992).

3.4. Anomalous tectonic subsidence

The ATS (Fig. 8) is calculated by subtracting the total tectonic subsidence derived from crustal extension (Fig. 7) from the total tectonic subsidence estimated from the sediment thickness (Fig. 6) in each given basin. The difference illustrates the degree of ATS of a given basin (Fig. 8). The global median value for the selected basins of this study is 1.37 km of ATS.

Apart from the eastern Chinese Basins, the Basin and Range Province, and the Patagonian offshore region, the overwhelming majority of the basins shows large ATS values (Fig. 8). This is due to larger tectonic subsidence estimates from the sediment thickness, than from crustal stretching. In basins with higher sediment densities, for example due to significant carbonate deposition, a part of the large ATS values is probably due to an underestimation of the average densities as compared to Sykes (1996) equation. Potentially, this is to be expected for the Arabian Peninsula. In order to quantify the error due to generalising the sediment densities, more detailed local assessments are required which go beyond the scope of this global study.

The anomalous tectonic subsidence (Fig. 8) does not discriminate between mechanisms other than crustal stretching which can create sediment accommodation space, such as flexural loading or

Please cite this article in press as: Heine, C., et al., Subsidence in intracontinental basins due to dynamic topography, Phys. Earth Planet. Interiors (2008), doi:10.1016/j.pepi.2008.05.008

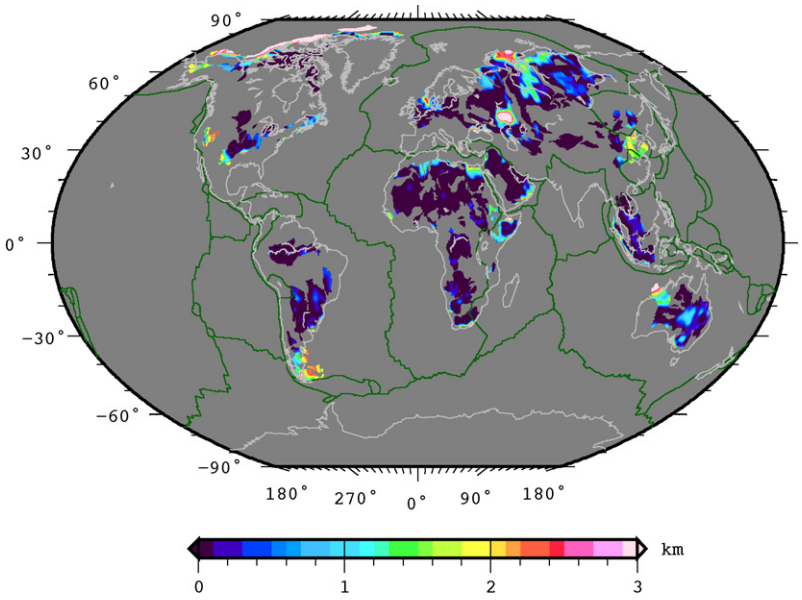

Fig. 7. Global map of total tectonic subsidence derived from crustal extension factors for selected basins of this study. As the calculated TTS_{cru} is based on the computed crustal extensional factor, the patterns observed in the map are very similar. The highest SBCT tectonic subsidence can be found in the Precaspian, the northern, passive margin part of the West Siberian Basin and the Canning basin, the Patagonian Basins of South America and some North American Arctic Basins.

magmatic intrusions. In basins close to convergent plate boundaries, like the northern part of the Arabian basins, or the Tarim Basin, flexural effects can be the dominating cause for anomalously high tectonic subsidence values.

4. Deep-Earth dynamics, plate kinematics, crustal structure and subsidence of intracontinental basins

First and second order mantle convection patterns have long been recognised as a mechanism that is able to create or destroy sediment accommodation space and control the large-scale flooding patterns of continents (Lithgow-Bertelloni and Gurnis, 1997; Burgess and Gurnis, 1995; Gurnis, 1993). However, due to a lack of frameworks which allow the integration and combined analysis of mantle convection, plate kinematics and crustal structure, the amplitude and spatial effects of dynamic topography on the subsidence of intracontinental basins has not been quantified in the past. For conventional basin modelling, its effects are usually not taken into account, partly due to the lack of a widely accepted, calibrated dynamic topography model and partly because of the common perception that these effects are negligible for industry-standard basin modelling.

4.1. Dynamic subsidence

We have analysed the plate kinematics and Cenozoic dynamic topography history for a global set of intracontinental basins (Fig. 9) in order to quantify the vertical changes induced by the relative

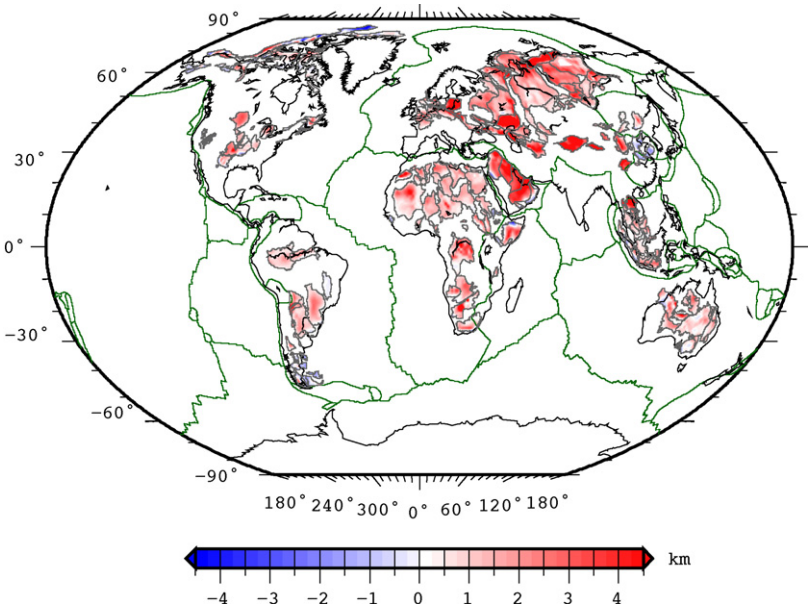

Fig. 8. Global anomalous tectonic subsidence for selected basins. Red colours indicate larger tectonic subsidence computed from sediment thickness than from crustal thickness, blue colours indicate the opposite. Note that most younger extensional tectonic systems like the East African rift, the Patagonian South Atlantic basins, the eastern Chinese Basins have low anomalous tectonic subsidence values. Grid cell size is $2' \times 2'$.

Please cite this article in press as: Heine, C., et al., Subsidence in intracontinental basins due to dynamic topography, Phys. Earth Planet. Interiors (2008), doi:10.1016/j.pepi.2008.05.008

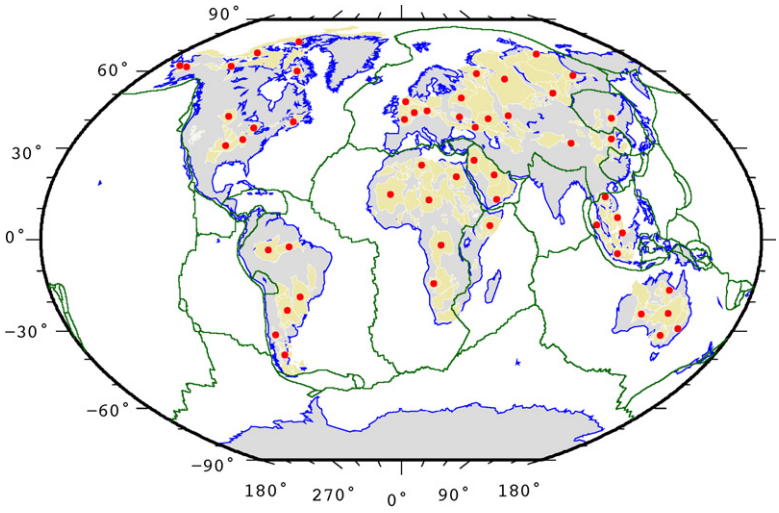

Fig. 9. Global basin data set and basin centroids (red dots) for selected basin polygons where dynamic topography signal is extracted.

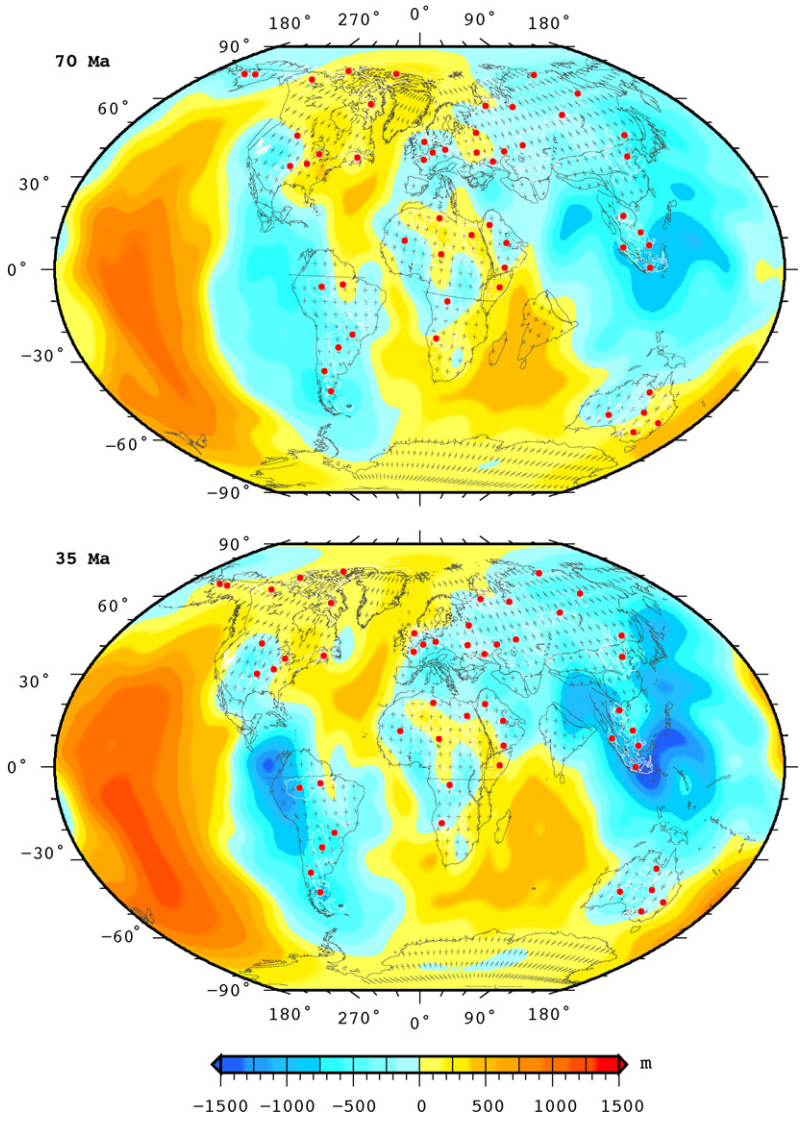

Fig. 10. Absolute plate reconstructions and dynamic topography models with intracontinental basin polygons superimposed for 70 Ma (top) and 35 Ma (bottom). Centroids of 54 selected basin polygons are plotted as red dots. Dynamic topography model based on S20RTS model (Ritsema et al., 2004, 1999). Past plate positions based on EarthByte plate kinematic framework (Müller et al., 2008b, a). For present-day configuration see Fig. 3.

Please cite this article in press as: Heine, C., et al., Subsidence in intracontinental basins due to dynamic topography, Phys. Earth Planet. Interiors (2008), doi:10.1016/j.pepi.2008.05.008

position of the basins with respect to the large-scale patterns of mantle convection. The individual centroid of a basin polygon is used as reference point. These center points are then rotated back to their past position using the EarthByte plate model (Fig. 10), and dynamic topography amplitudes are extracted from the analytical flow model. This allows to reconstruct the dynamic topography history of selected basins in 1 Myr time steps from 70 Ma to the present (Fig. 11). Out of the total 229 basins from our global basin database we have chosen 54 basins scattered over 11 regions (Fig. 9, red dots) where we extracted a detailed dynamic topography history (Fig. 11).

The data generally illustrate that most intracontinental basins have experienced mantle convection-induced net "dynamic subsidence" during the Cenozoic (Figs. 10 and 11). The observed pattern reflects the disintegration of the supercontinent Pangaea, which started in the Jurassic and continues until today. As the current plate tectonic configuration reflects one of continental dispersal, most of the continental plates have migrated towards zones of long-lasting subduction (Figs. 3 and 10; Anderson, 1994). Regions or continents which remained stationary during the Cenozoic show little net dynamic subsidence, or even uplift, like the Somali Basin in north-eastern Africa in the vicinity of the East African Rift (Fig. 11a) or Europe (Fig. 11f).

Stable, broad downwellings dominate the pattern of convection over relatively weaker upwellings and plumes (Bercovici et al., 2000). The regions which have been situated close to, or above mantle downwellings during the Cenozoic show very uniform dynamic subsidence patterns (e.g. Siberia, Fig. 11j; the Caspian, Fig. 11d; China, Fig. 11e), confirming the large spatial extent of the broad belts of negative dynamic topography and their relative stability. Regions which moved towards these prominent zones from a relative dynamic topography high, like the Australian (Fig. 11c), North American (Fig. 11g), South American Plates (Fig. 11i) display the largest amounts of dynamic subsidence due to the displacement of the plates relative to the underlying convection cells. Absolute dynamic topography amplitudes are largest in Southeast Asia (Fig. 11k), because the region is located above the convergence of two major subduction zones (Tethys/Indian Ocean and Pacific) which have existed for at least 140 Myr (Metcalfe, 1991).

The African plate contains many old, cratonic basins (Hartley and Allen, 1994; Burke et al., 2003) and occupied a central position in the Pangaea supercontinent. It has moved only little northward in an absolute plate motion reference frame during the Cenozoic and hence only experienced minor displacement relative to the underlying convection patterns. Insulation effects supercontinent assemblages (Anderson, 1994; Lenardic et al., 2005), and the distal position relative to major downwellings and subduction zones prevented the African continent from being affected by major negative dynamic topography during the Cenozoic. Basins in Southern Africa experienced uplift due to increasing positive dynamic topography (Fig. 11a; Gurnis et al., 2000; Lithgow-Bertelloni and Silver, 1998). Northward motion of Africa towards the Tethyan subduction-related mantle downwelling resulted in increasing negative dynamic topography since the Miocene for most northern and central African basins (Fig. 11a). Most likely this would have lowered the topographic base level and generated additional accommodation space. When comparing predicted and observed topography with crustal structure data, Mooney and Vidale (2003) found that the "residual topography unexplained by crust" for most of the north-western African basins (e.g. Taoudeni, Chad, Ghadames Basin) shows elevations too low compared to what would be expected from their respective crustal thicknesses. Dynamic topography profiles from the Arabian basins (Fig. 11b) indicate that the region has experienced negative dynamic topography for the Cenozoic, with a relatively sharp increase in amplitude during the last 20 Myr. This suggests not only that anomalous subsidence stored in the Arabian basins would have been relatively protected from erosion and isostatic rebound, but also that the region has been susceptible to Cenozoic flooding and sediment deposition due to a lowered topographic base level by negative dynamic topography.

Most Australian basins have experienced a large increase in negative dynamic topography during the last 70 Myr (Fig. 11c). Starting with positive dynamic topography in the Paleogene, Australia's Cenozoic northward motion towards the Southeast Asian mantle downwelling resulted in increasing negative topography. In combination with falling sea levels, this would have resulted in higher exposure of the Australian basins during the Late Cretaceous and early Tertiary, with a progressive lowering of the topographic base level from about 30 Ma to the present, making the basin areas more susceptible to flooding and preventing erosion (Heine et al., in revision).

The Caspian Basins (Fig. 11d) experienced a similar geodynamic evolution as the Arabian basins, with neutral to slightly negative dynamic topography. This likely prevented erosion and favoured deposition in times of higher sea levels in the early Tertiary. Increasing negative dynamic topography in conjunction with falling sea levels kept the topographic base level low, likely preventing erosion. The Precaspian basin, as one of the deepest sedimentary basins of the planet, has likely been situated above a mantle downwelling since the Triassic (Stampfli and Borel, 2002; Golonka, 2004) and experienced little deformation through crustal extension in this time (Brunet et al., 1999; Volozh et al., 2003; Brunet et al., 2003). However, large thicknesses (about 15 km) of sediments accumulated in Mesozoic–Cenozoic times. We attribute this to the position of the Precaspian basin relative to the large-scale mantle downwelling induced by subduction of Tethyan ocean lithosphere beneath the southern Eurasian margin. The extreme sediment thicknesses with the constant negative topography might have triggered mineral phase transitions due to the overburden (Kaus et al., 2005; Petrini et al., 2001), which could have significantly increased the lithospheric densities and further influenced the isostatic response of the basin. A large mismatch of elevation and crustal structure for the Caspian region is reported by Mooney and Vidale (2003).

Long-lasting subduction of Pacific Ocean lithosphere beneath Far East Asia feeds one of the largest observed zones of mantle downwelling on Earth (Fig. 3). Thus the Chinese Basins (Fig. 11e) show negative dynamic topography for the Cenozoic with a slight increase within the last 10–20 Myr. This would suggest a constant lowering of the topographic base level and a larger likelihood of flooding of low-lying basins during the Neogene. However, the geodynamic evolution of the area is complicated due to the proximity to plate boundaries and tectonic events affecting the region.

The European Basins (Fig. 11f) show neutral to low negative dynamic topography throughout the Cenozoic, likely causing enough deflection of the surface to prevent erosion of accumulated "anomalous" sediment thickness. Since the late Miocene, negative dynamic topography increased little, probably lowering much of the topographic base level in Central Europe (e.g. North German Basin), related to a slight southward motion of Europe towards the mantle downwelling of the Tethyan subduction.

Many North American (Fig. 11g) and the Arctic basins (Fig. 11h) have experienced a change in dynamic topography from about neutral to positive to slightly negative dynamic topography during the Cenozoic. For basins with anomalous sediment accumulation this would have resulted in non-deposition and/or erosion and, again, a lowering of topographic base level since about 30 Ma, making topographically low-lying basins susceptible to flooding even with falling eustatic sea level.

Please cite this article in press as: Heine, C., et al., Subsidence in intracontinental basins due to dynamic topography, Phys. Earth Planet. Interiors (2008), doi:10.1016/j.pepi.2008.05.008

Intracontinental basins of South America (Fig. 11i) reflect the global trend with an increase of negative dynamic topography throughout the Cenozoic. Observed dynamic topography amplitudes for most basins are large, likely due to the relative motion of the South American continent towards and over the long-established subduction-related mantle downwelling along the eastern Pacific margin. Large negative dynamic topography amplitudes would also explain the "unexplained topography" in much of South America of Mooney and Vidale (2003) and particularly make the south-eastern South American basins susceptible to flooding and deposition throughout the Cenozoic.

Basins in most of Far Eastern Russia (Fig. 11j) show an increasing negative dynamic topography over the last 70 Myr, counterbalancing the effect of a falling eustatic sea level. There-

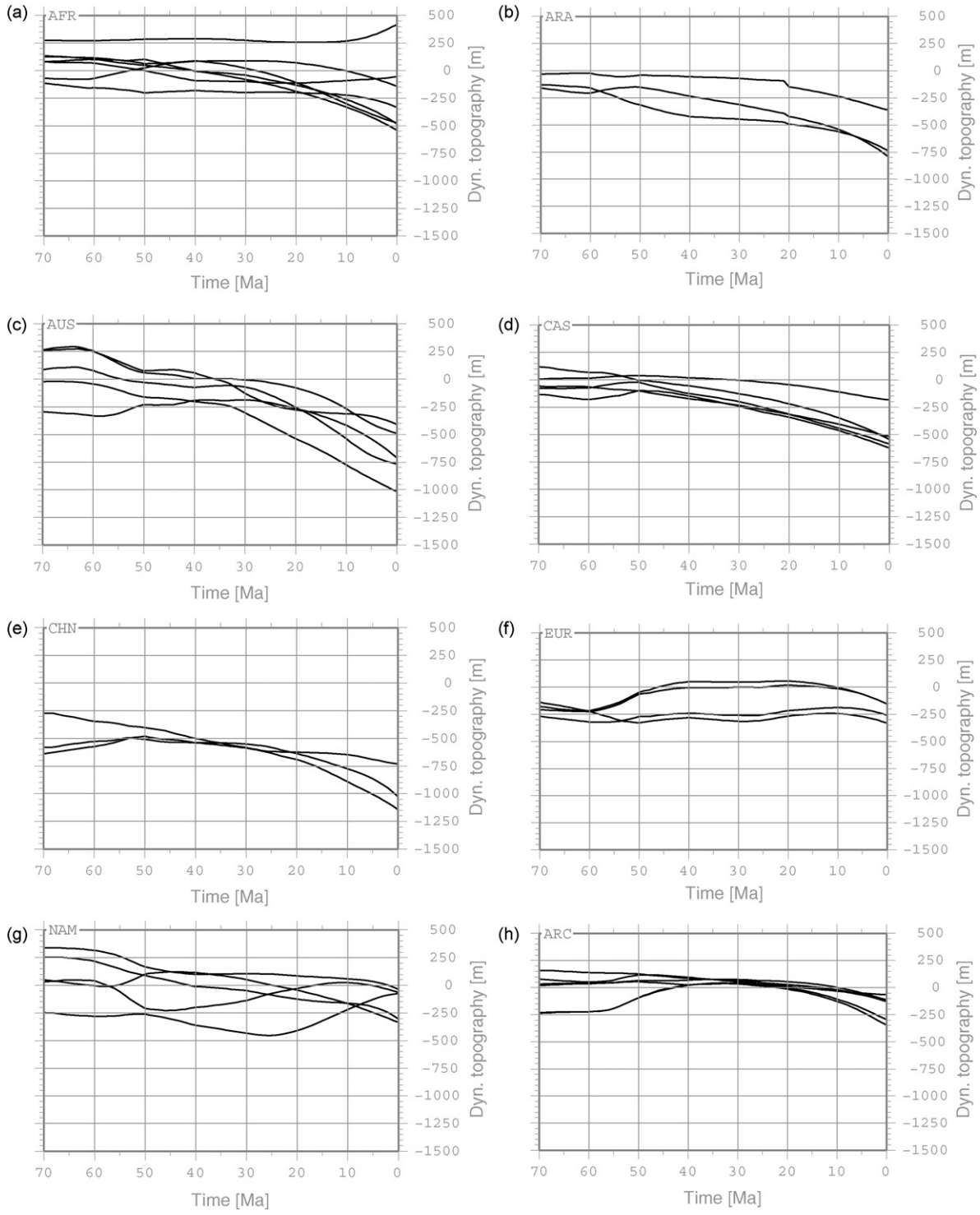

Fig. 11. Dynamic topography history for 54 selected basin polygons centroids for the last 70 Myr by region. Dynamic topography based on S20RTS model (Ritsema et al., 2004, 1999). Region grouping according to Fig. 1 with AFR, African Basins; ARA, Arabian Basins; AUS, Australian Basins; CAS, Greater Caspian region; CHN, Chinese Basins; EUR, European basins; NAM, North American Basins; ARC, Arctic North American Basins; SAM, South American Basins; SIB, Siberian Basins; SUN, Sundaland Basins.

Please cite this article in press as: Heine, C., et al., Subsidence in intracontinental basins due to dynamic topography, Phys. Earth Planet. Interiors (2008), doi:10.1016/j.pepi.2008.05.008

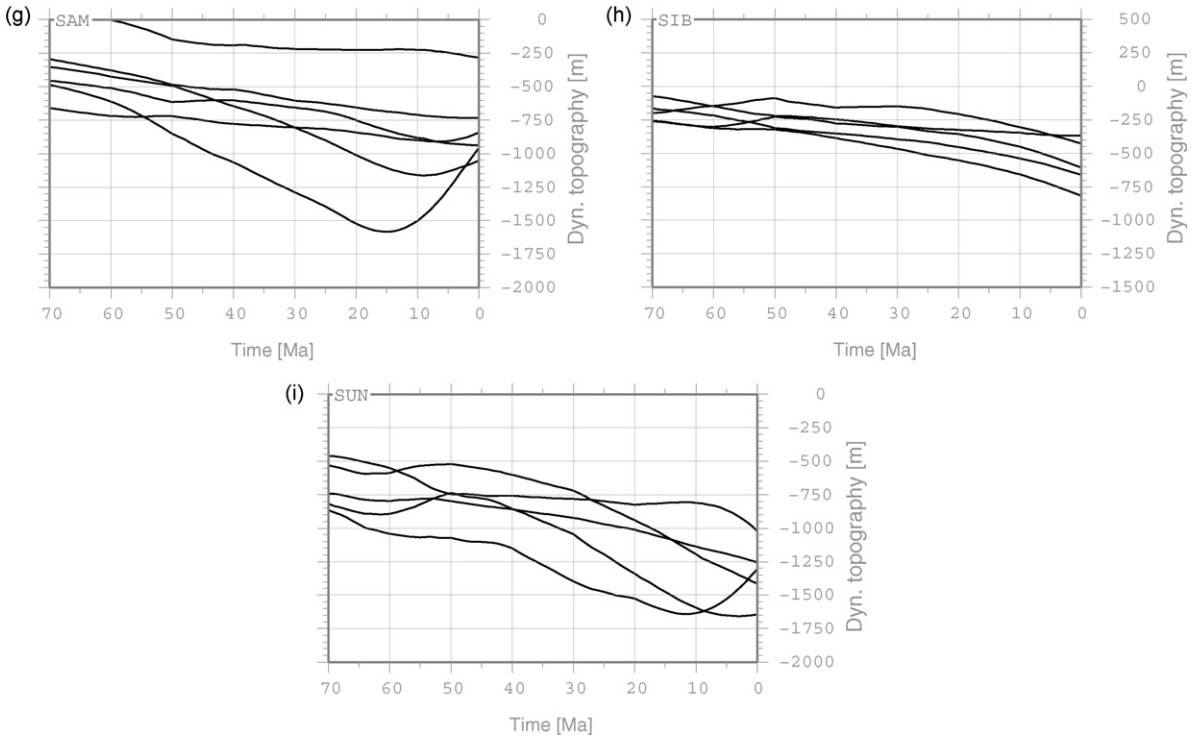

Fig. 11. (*Continued*).

fore anomalous subsidence in the Siberian basins is most likely preserved throughout the Cenozoic with additional continued deposition in low-lying basins, like the northern part of the WSB and adjacent basins.

In Sundaland (Fig. 11k), the convergence of Pacific and Tethyan/Indo-Australian plates have created one of the broadest areas of mantle downwelling, hence the dynamic topography history of the Southeast Asian basins shows the largest negative dynamic topography amplitudes. This suggests, that throughout the Cenozoic the basins provide additional sediment accumulation space, resulting in anomalous tectonic subsidence. The proximity to active plate boundaries may, however, prohibit a direct correlation between the effects of mantle downwelling and increased sedimentation, although Morley and Westaway (2006) report extremely high, anomalous post-rift subsidence values (6–12 km) from the Pattani-Malay basins. Hall and Morley (2004) report many deep, rapidly subsiding Cenozoic basins from the Sundaland part of Southeast Asia where there are problems in "understanding the origin of the stresses driving them, and the amount of sediment accumulated."

4.2. Dynamic versus anomalous tectonic subsidence

Linking integrated Cenozoic dynamic subsidence with anomalous tectonic subsidence computed from the global basin analysis provides important insight on the geodynamics of intracontinental basins but remains a challenging task. It requires a detailed analysis of the individual Cenozoic sedimentation record of each basin. However, the modeled dynamic topography evolution for selected global basin centroids (Fig. 11) allows to make assumptions on the contribution of mantle convection-induced vertical motions to the Cenozoic subsidence history of the individual basins. The anomalous tectonic subsidence does not contain time information and is integrated over the basin lifespan. The dynamic topography history in contrast is limited to the last 70 Myr.

By using the age of the basin as determined by the basement we can discriminate correlation patterns in the dynamic subsidence versus ATS. Basins with age information in our database were selected based on whether they are still locus of sediment deposition, meaning the young basin age is 0 Ma. Using the basement age as indication for the start of sedimentation, the selected basins were grouped in two different age ranges (less than 100 Myr old and 100–250 Myr old; Fig. 12). We applied a spline-fitting algorithm (Thijsse et al., 1998) to investigate trends in the data.

For selected basins less than 100 Myr old we cannot derive a clear relationship between ATS and dynamic subsidence integrated over the last 70 Myr. However, apart from one exception, all selected basins plot in the upper right quadrant of the ATS versus net dynamic subsidence graph (Fig. 12a). This reflects than ATS is paired with predicted negative dynamic topography. However, a clear linear trend between ATS and dynamic subsidence integrated over the last 70 Myr is lacking. The data points form a cloud centered around 750 m net dynamic subsidence and about 500 m of ATS.

The lack of a clear trend in the "young" basins group (Fig. 11a) can be explained by the following reasons: First, the basins in this group are almost exclusively located on the stable Sundaland core in SE Asia (Hall and Morley, 2004; Hall, 1998), two out of 20 are located in Africa and one basin in Australia. SE Asia is affected by a major downwelling caused by the convergence and subduction of the Pacific and Indian Ocean plates resulting in large negative dynamic topography amplitudes (Fig. 11k; Lithgow-Bertelloni and Gurnis, 1997). Additionally, most of the basin polygons in SE Asia have a small to medium size (mean of 86053 km^2) compared to other regions. These basin polygon sizes are well below the original spatial resolution of 2° for the crustal data sets. Thus sediment thicknesses for those basins might be drastically underestimated. Lastly, basins less than 100 Myr old are likely not fully thermally equilibrated and will continue to show ongoing thermal subsidence. Lastly, some of the SE Asian basins are likely affected by

Please cite this article in press as: Heine, C., et al., Subsidence in intracontinental basins due to dynamic topography, Phys. Earth Planet. Interiors (2008), doi:10.1016/j.pepi.2008.05.008

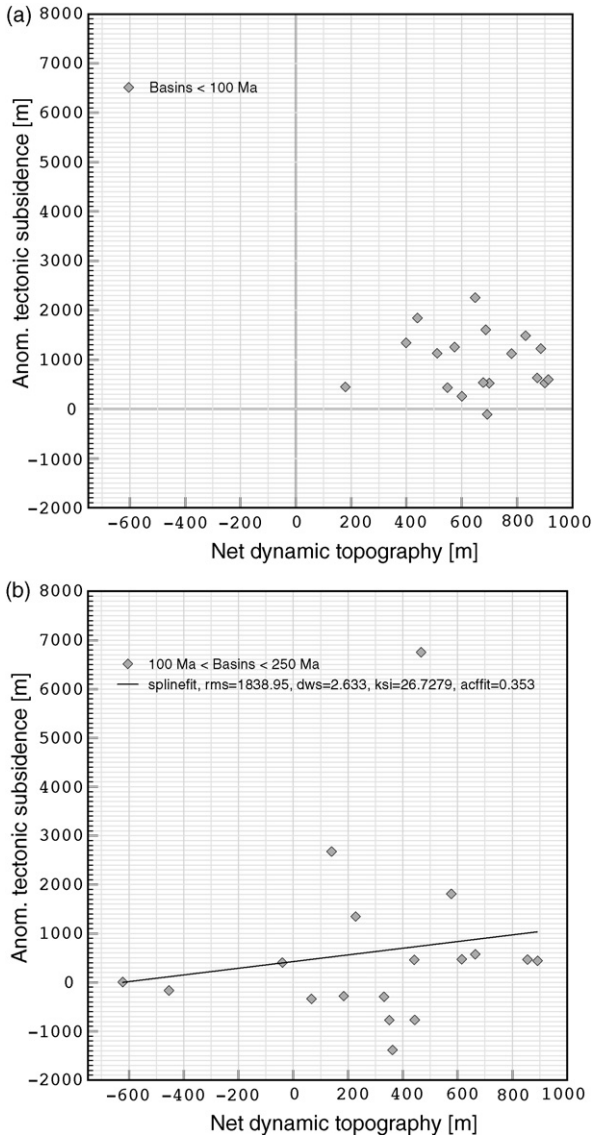

Fig. 12. Net dynamic topography for the last 70 Myr versus anomalous tectonic subsidence for basin polygons grouped by basin age for basins less than 100 Myr old (a) and "Mesozoic" basins 100 to 250 Myr old (b). Positive values on y-axis indicate anomalous subsidence, positive numbers on x-axis indicate dynamic subsidence, negative numbers indicate dynamic uplift. Dynamic topography model based on S20RTS seismic tomography (Ritsema et al., 2004, 1999). We used a spline-fitting algorithm (Thijsse et al., 1998) to derive the correlation between the data. Abbreviations: rms, root mean square of the noise amplitude data; DWS, Durbin–Watson statistic for the fitted spline (values between 1.9 and 2.2 usually indicate a good fit); ksi, autocorrelation length ξ; acffit, measure of how closely the autocorrelation function of the fit-residuals matches the assumed autocorrelation function with autocorrelation length ξ.

localised tectonic deformation which might have a similar, if not larger impact on the subsidence. As our approach only takes the total amount of accumulated sediment into account, we are not able to discriminate these effects on the subsidence signal.

For selected basin centroids of Mesozoic-aged basins (Fig. 12b) we find a relationship of about 1:1.5 of ATS versus net dynamic subsidence as indicated by linear spline-fitted trends. The basin centroids in this plot reflect much broader regional distribution (8 out of 12 regions) and basin sizes are much larger (mean of 324,593 km^2) as opposed to the basins less than 100 Myr old. Furthermore, the "Mesozoic" basins are likely fully thermally equilibrated and thus the trend can be regarded as robust.

5. Discussion

We have shown that anomalous tectonic subsidence in intracontinental basins is likely caused by basins moving to regions of negative dynamic topography due to the continuing dispersal of the supercontinent Pangaea. By using an analytical flow model to compute time-dependent dynamic topography based on the S20RTS seismic tomography model (Ritsema et al., 1999) in conjunction with global plate kinematics, we track the vertical motions for a global set of 229 basin polygons over the last 70 Ma. Most intracontinental basins in a stable tectonic setting show a history of subsidence and the creation of additional sediment accommodation space due to plate motion towards mantle downwellings. Utilising ATS as a parameter derived from a global crustal structure analysis, we can quantify the amount of basin subsidence not related to crustal extension. Our results indicate generally a positive correlation between the sediment- and crustal structure-derived ATS and predicted net dynamic subsidence for our selected basins.

As our analysis of anomalous tectonic subsidence considers the total sediment thickness in each given basin, it is time-independent. Due to the limitations of the backward-advection model, the study only covers the last 70 Myr of dynamic topography history. A direct correlation between sediment accumulation as reflected in the basin stratigraphy and dynamic subsidence hence requires access to detailed stratigraphic data and will be the focus of future work. We propose that phase changes triggered by increasing overburden (Artyushkov, 2007; Kaus et al., 2005; Petrini et al., 2001) due to continued negative dynamic topography might cause anomalous tectonic subsidence to be "stored" in a given sedimentary basin.

Competing mechanisms which might also contribute to anomalous tectonic subsidence are magmatic intrusions during the initial extensional phase of a given basin or changes in the large-scale stress field (e.g. Birt et al., 1997; Lyngsie et al., 2007; Marotta et al., 2000). Although these effects might operate on shorter wavelengths, they will contribute to the anomalous tectonic subsidence resolved with our method.

The methodology outlined in this paper is extremely dependent on the accuracy and resolution of crustal structure data. Therefore basin sizes below the original grid resolution of the CRUST2 model are not well constrained in terms of their anomalous tectonic subsidence. Future developments in numerical modelling and seismic tomography model resolution will enable greater accuracy of our prediction in combination with better stratigraphic control on basin level.

The data presented in this study are accessible online through the ICONS interactive atlas as part of the EarthByte portal (http://www.earthbyte.org/resources/ICONS/index.html).

Acknowledgements

We are grateful for constructive reviews and comments by Philip Allen and Hans Thybo as well as Taras Gerya, the editor of this special edition. All helped to significantly improve the original version of the manuscript. Maria Sdrolias is acknowledged for supplying the paleo-positions of global subduction zones. Figures for this paper were almost exclusively generated using the Generic Mapping Tools (Wessel and Smith, 1998).

References

Allen, P.A., Allen, J.R., 2005. Basin Analysis: Principles and Applications, 2nd Edition. Blackwell Publishing, Incorporated, Oxford, United Kingdom.
Anderson, D.L., 1994. Superplumes or supercontinents. Geology 22, 39–42.

Artyushkov, E.V., 1992. Role of crustal stretching on subsidence of the continental crust. Tectonophysics 215 (1–2), 187–207.
Artyushkov, E.V., 2007. Formation of the superdeep South Caspian basin: subsidence driven by phase change in continental crust. Russ. Geol. Geophys. 48 (12), 1002–1014.
Bassin, C., Laske, G., Masters, G., 2000. The current limits of resolution for surface wave tomography in North America. EOS Trans. Am. Geophys. Union 81, 897.
Bercovici, D., Ricard, Y., Richards, M.A., 2000. The relation between mantle dynamics and plate tectonics: a primer. In: Richards, M.A., Gordon, R.G., van der Hilst, R.D. (Eds.), The History and Dynamics of Global Plate Motions, Geophysical Monograph Series, Vol 121. American Geophysical Union, pp. 5–46.
Bird, P., 2003. An updated digital model of plate boundaries. Geochem. Geophys. Geosyst. 4 (3), 1027, doi:10.1029/2001GC000252.
Birt, C.S., Maguire, P.K.H., Khan, M.A., Thybo, H., Keller, G.R., Patel, J., 1997. The influence of pre-existing structures on the evolution of the southern Kenya Rift Valley—evidence from seismic and gravity studies. Tectonophysics 278 (1-4), 211–242.
Bond, G., 1976. Evidence for continental subsidence in North America during the Late Cretaceous global submergence. Geology 4, 557–560.
Bond, G.C., 1978. Speculations on real sea-level changes and vertical motions of continents at selected times in the Cretaceous and Tertiary periods. Geology 6, 247–250.
Brunet, M.F., Korotaev, M.V., Ershov, A.V., Nikishin, A.M., 2003. The South Caspian Basin: a review of its evolution from subsidence modelling. Sed. Geol. 156, 119–148.
Brunet, M.F., Volozh, Y.A., Antipov, M.P., Lobkovsky, L.I., 1999. The geodynamic evolution of the Precaspian Basin (Kazakhstan) along a north-south section. Tectonophysics 313, 85–106.
Burgess, P.M., Gurnis, M., 1995. Mechanisms for the formation of cratonic stratigraphic sequences. Earth Planet. Sci. Lett. 136, 647–663.
Burke, K., MacGregor, D.S., Cameron, N.R., 2003. Africa's petroleum systems: four tectonic "aces" in the past 600 million years. In: Arthur, T., MacGregor, D.S., Cameron, N.R. (Eds.), Petroleum geology of Africa: new themes and developing techniques, No. 207 in Geological Society Special Publication. Geological Society of London, London, United Kingdom, pp. 21–60.
Conrad, C.P., Gurnis, M., 2003. Seismic tomography, surface uplift, and the breakup of Gondwanaland: Integrating mantle convection backwards in time. Geochem. Geophys. Geosyst. 4 (3), 1031, doi:10.1029/2001GC000299.
Davies, G.F., 1999. Dynamic Earth—Plates, Plumes and Mantle Convection. Cambridge University Press.
Exxon Production Research Company, 1985. Tectonic Map of the World. American Association of Petroleum Geologists Foundation, Tulsa, OK, USA.
Golonka, J., 2004. Plate tectonic evolution of the southern margin of Eurasia in the Mesozoic and Cenozoic. Tectonophysics 381, 235–273.
Grand, S.P., van der Hilst, R.D., Widiyantoro, S., 1997. Global seismic tomography; a snapshot of convection in the Earth. GSA Today 7 (4), 1–7.
Gurnis, M., 1990. Bounds on global dynamic topography from Phanerozoic flooding of continental platforms. Nature 344, 754–756.
Gurnis, M., 1993. Phanerozoic marine inundation of continents driven by dynamic topography above subducting slabs. Nature 364, 589–593.
Gurnis, M., 2001. Sculpting the Earth from inside out. Sci. Am. 284, 40–48.
Gurnis, M., Mitrovica, J.X., Ritsema, J., van Heijst, H.J., 2000. Constraining mantle density structure using geological evidence of surface uplift rates: the case of the African superplume. Geochem. Geophys. Geosyst., 1.
Gurnis, M., Müller, R.D., Moresi, L.N., 1998. Cretaceous vertical motion of Australia and the Australian–Antarctic discordance. Science 279, 1499–1504.
Gurnis, M., Zhong, S., 1991. Generation of long-wavelength heterogeneity in the mantle by the dynamic interaction between plates and convection. Geophys. Res. Lett. 18, 581–584.
Hager, B.H., O'Connell, R.J., 1981. A simple global model of plate dynamics and mantle convection. J. Geophys. Res. 86, 4843–4867.
Hall, R., 1998. The plate tectonics of Cenozoic SE Asia and the distribution of land and sea. In: Hall, R., Holloway, J.D. (Eds.), Biogeography and Geological Evolution of SE Asia. Blackhuys Publisher, Leiden, pp. 99–131.
Hall, R., Morley, C.K., 2004. Sundaland Basins. In: Clift, P., Hayes, D., Kuhnt, W., Wang, P. (Eds.), Continent-Ocean Interactions within East Asian Marginal Seas, Geophysical Monograph Series, Vol. 149. American Geophysical Union, Washington D.C., USA, pp. 55–85.
Hartley, R.W., Allen, P.A., 1994. Interior cratonic basins of Africa: relation to continental break-up and the role of mantle convection. Basin Res. 6, 65–113.
Heine, C., Müller, R. D., Steinberger, B., DiCaprio, L. Integrating deep Earth dynamics in paleogeographic reconstructions of Australia. Palaeogeogr. Palaeoclimatol. Palaeoecol., submitted for publication.
Karato, S., 1993. Importance of anelasticity in the interpretation of seismic tomography. Geophys. Res. Lett. 20, 1623–1626.
Kaus, B.J.P., Connolly, J.A.D., Podladchikov, Y.Y., Schmalholz, S.M., 2005. Effect of mineral phase transitions on sedimentary basin subsidence and uplift. Earth Planet. Sci. Lett. 233, 213–228, doi:10.1016/j.epsl.2005.01.032.
Khain, V.Y., 1992. The role of rifting in the evolution of the Earth's crust. Tectonophysics 215 (1–2), 1–7.
Kingston, D.R., Dishroon, C.P., Williams, G.D., 1983. Global basin classification system. AAPG Bull. 67 (12), 2175–2193.
Klein, G.D., 1995. Intracratonic Basins. Blackwell Science, Cambridge, Massachusetts, Ch. Tectonics of Sedimentary Basins, 459–478.
Klemme, H.D., 1980. Petroleum basins: classification and characteristics. J. Petrol. Geol. 3 (2), 187–207.
Klemme, H.D., Ulmishek, G.F., 1991. Effective Petroleum Source Rocks of the World: Stratigraphic Distribution and Controlling Depositional Factors. AAPG Bull. 75, 1809–1851.
Kominz, M.A., Browning, J.V., Miller, Kenneth, G., Sugarman, J., Mizintsevaw, S., Scotese, C.R., 2008. Late Cretaceous to Miocene sea-level estimates from the New Jersey and Delaware coastal plain coreholes: an error analysis. Basin Res., 1–16.
Laske, G., 2004. A New Global Crustal Model at 2×2Degrees. URL: http://mahi.ucsd.edu/Gabi/rem.dir/crust/crust2.html.
Laske, G., Masters, G., 1997. A global digital map of sediment thickness. EOS Trans. Am. Geophys. Union 78, 483.
Le Pichon, X., Sibuet, J.C., 1981. Passive margins: a model of formation. J. Geophys. Res. 86, 3708–3720.
Lenardic, A., Moresi, L.N., Jellinek, A.M., Manga, M., 2005. Continental insulation, mantle cooling, and the surface area of oceans and continents. Earth Planet. Sci. Lett. 234 (3–4), 317–333.
Lithgow-Bertelloni, C., Gurnis, M., 1997. Cenozoic subsidence and uplift of continents from time-varying dynamic topography. Geology 25 (8), 735–738.
Lithgow-Bertelloni, C., Silver, P.G., 1998. Dynamic topography, plate driving forces and the African superswell. Nature, 395.
Lyngsie, S.B., Thybo, H., Lang, R., 2007. Rifting and lower crustal reflectivity: a case study of the intracratonic Dniepr-Donets rift zone, Ukraine. J. Geophys. Res. 112, 12402.
Marotta, A.M., Bayer, U., Thybo, H., 2000. The legacy of the NE German Basin: reactivation by compressional buckling. Terra Nova 12, 132–140.
McKenzie, D.P., 1978. Some remarks on the development of sedimentary basins. Earth Planet. Sci. Lett. 40, 25–32.
Metcalfe, I., 1991. Allochthonous terrane processes in Southeast Asia. In: Dewey, J.F., Gass, I.G., Curry, G.B., Harris, N.B.W., Şengör, A.M.Ç. (Eds.), Allochthonous Terranes. Cambridge University Press, pp. 169–184.
Milanovsky, E.E., 1992. Aulacogens and aulacogeosynclines: regularities in setting and evolution. Tectonophysics 215 (1–2), 55–68.
Mooney, W.D., Vidale, J.E., 2003. Thermal and chemical variations in subcrustal cratonic lithosphere: evidence from crustal isostasy. Lithos 71 (2–4), 185–193.
Morley, C.K., Westaway, R., 2006. Subsidence in the super-deep Pattani and Malay basins of Southeast Asia: a coupled model incorporating lower-crustal flow in response to post-rift sediment loading. Basin Res. 18, 51–84.
Müller, R.D., Sdrolias, M., Gaina, C., Roest, W.R., 2008a. Age, spreading rates, and spreading asymmetry of the world's ocean crust. Geochem. Geophys. Geosyst. 9 (4), Q04006.
Müller, R.D., Sdrolias, M., Gaina, C., Steinberger, B., Heine, C., 2008b. Long-term sea-level fluctuations driven by ocean basin dynamics. Science 319 (5868), 1357–1362.
O'Neill, C., Müller, D., Steinberger, B., 2005. On the uncertainties in hot spot reconstructions and the significance of moving hot spot reference frames. Geochem. Geophys. Geosyst. 6, 04003.
Petrini, K., Connolly, J.A.D., Podlachikov, Y., 2001. A coupled petrological-tectonic model for sedimentary basin evolution: the influence of metamorphic reactions on basin subsidence. Terra Nova 13, 354–359.
Ritsema, J., van Heijst, H.J., Woodhouse, J.H., 1999. Complex shear wave velocity structure imaged beneath Africa and Iceland. Science 286, 1925–1928.
Ritsema, J., van Heijst, H.J., Woodhouse, J.H., 2004. Global transition zone tomography. J. Geophys. Res. 109, 02302.
Sawyer, D.S., 1985. Total tectonic subsidence: a parameter for distinguishing crust type at the U.S. Atlantic Continental Margin. J. Geophys. Res. 90 (B9), 7751–7769.
Şengör, A.M.Ç., 1995. Sedimentation and tectonics of fossil rifts. In: Ingersoll, R.V., Busby, C.J. (Eds.), Tectonics of Sedimentary Basins. Blackwell Science, pp. 53–117.
Sleep, N.H., 1976. Platform subsidence mechanisms and "eustatic" sea-level changes. Tectonophysics 36 (1–3), 45–56.
Sloss, L.L., 1963. Sequences in the cratonic interior of North America. Geol. Soc. Am. Bull. 74, 93–114.
Spasojevic, S., Liu, L., Gurnis, M., Müller, R.D., 2008. The case for dynamic subsidence of the U.S. east coast since the Eocene. Geophys. Res. Lett. 35, 08305.
Stampfli, G.M., Borel, G.D., 2002. A plate tectonic model for the Paleozoic and Mesozoic constrained by dynamic plate boundaries and restored synthetic oceanic isochrons. Earth Planet. Sci. Lett. 196, 17–33.
Steinberger, B., 2007. Effects of latent heat release at phase boundaries on flow in the Earth's mantle, phase boundary topography and dynamic topography at the Earth's surface. Phys. Earth Planet. Int. 164, 2–20.
Steinberger, B., Calderwood, A.R., 2006. Models of large-scale viscous flow in the Earth's mantle with constraints from mineral physics and surface observations. Geophys. J. Int. 167, 1461–1481.
Steinberger, B., Schmeling, H., Marquart, G., 2001. Large-scale lithospheric stress field and topography induced by global mantle circulation. Earth Planet. Sci. Lett. 186, 75–91.
Steinberger, B., Sutherland, R., O'Connell, R.J., 2004. Prediction of Emperor-Hawaii seamount locations from a revised model of global plate motion and mantle flow. Nature 430, 167–173.
Sykes, T.J.S., 1996. A correction for sediment load upon the ocean floor: uniform versus varying sediment density estimations–implications isostatic correction. Mar. Geol. 133, 35–49.

Please cite this article in press as: Heine, C., et al., Subsidence in intracontinental basins due to dynamic topography, Phys. Earth Planet. Interiors (2008), doi:10.1016/j.pepi.2008.05.008

Thijsse, B.J., Hollanders, M.A., Hendrikse, J., 1998. A partical algorithm for least-squares spline approximation of data containing noise. Comput. Phys. 12 (4), 393–399.
Turcotte, D.L., Schubert, G., 2001. Geodynamics: Applications of Continuum Mechanics to Geological Problems, 2nd Edition. Cambridge University Press, Cambridge, United Kingdom.
Volozh, Y.A., Antipov, M.P., Brunet, M.-F., Garagash, I.A., Lobkovsky, L.I., Cadet, J.-P., 2003. Pre-Mesozoic geodynamics of the Precaspian Basin (Kazakhstan). Sed. Geol. 156, 35–58.
Vyssotski, A.V., Vyssotski, V.N., Nezhdanov, A.A., 2006. Evolution of the West Siberian Basin. Mar. Petrol. Geol. 23, 93–126.
Watts, A.B., 2001. Isostasy & Flexure of the Lithosphere, 1st Edition. Cambridge University Press, Cambridge, United Kingdom.
Wessel, P., Smith, W.H.F., 1998. New, improved version of Generic Mapping Tools released. EOS Trans. Am. Geophys. Union 79 (47), 579.
Xie, X., Müller, R.D., Lia, S., Gong, Z., Steinberger, B., 2006. Origin of anomalous subsidence along the Northern South China Sea margin and its relationship to dynamic topography. Mar. Petrol. Geol. 23, 745–765.

Please cite this article in press as: Heine, C., et al., Subsidence in intracontinental basins due to dynamic topography, Phys. Earth Planet. Interiors (2008), doi:10.1016/j.pepi.2008.05.008